



# Quantifying the aerosol effect on droplet size distribution at cloud-top

Lianet Hernández Pardo<sup>1</sup>, Luiz Augusto Toledo Machado<sup>1</sup>, Micael Amore Cecchini<sup>1,2</sup>, and Madeleine Sánchez Gácita<sup>1</sup>

<sup>1</sup>Centro de Previsão de Tempo e Estudos Climáticos, Instituto Nacional de Pesquisas Espaciais, Cachoeira Paulista, Brasil

<sup>2</sup>Departamento de Ciências Atmosféricas, Instituto de Astronomia, Geofísica e Ciências Atmosféricas, Universidade de São Paulo, Brasil

*Correspondence to:* Lianet Hernández Pardo ([lianet.pardo@inpe.br](mailto:lianet.pardo@inpe.br))

**Abstract.** This work uses the number concentration-effective diameter phase-space to test cloud sensitivity to variations in the aerosol population characteristics, such as the aerosol size distribution, number concentration and hygroscopicity. It is based on the information from the top of a cloud simulated by a bin-microphysics single-column model, for initial conditions typical of the Amazon. It is shown that the cloud-top evolution can be very sensitive to aerosol properties, but the relative importance of each parameter is variable. The sensitivity to each aerosol characteristic varies as a function of the tested parameter and is conditioned by the base values of the other parameters. The median radius of the aerosols showed the largest influence on this sensitivity. We show that all aerosol properties can have significant impacts on cloud microphysics, especially if the median radius of the aerosol size distribution is smaller than  $0.05 \mu\text{m}$ .

## 1 Introduction

Because of their role as cloud condensation nuclei (CCN) and ice nucleating particles, aerosols can affect the cloud optical properties (Twomey, 1974) and determine the onset of precipitation (Albrecht, 1989; Braga et al., 2017; Rosenfeld et al., 2008; Seifert and Beheng, 2006) and ice formation (Andreae et al., 2004; Fan et al., 2007; Gonçalves et al., 2015; Khain et al., 2005; Koren et al., 2010; Lee et al., 2008; Li et al., 2011). Aerosols also play an indirect role in the thermodynamics of local cloud fields through the suppression of cold pools and enhancement of atmospheric instability (Heiblum et al., 2016). However, knowledge about the characteristics of the effects of atmospheric aerosols on clouds and precipitation is still lacking and remains an important source of uncertainty in meteorological models.

Many studies have been dedicated to quantifying the effect of aerosols on clouds through sensitivity calculations, using both modeling and observational approaches. Knowing the real values of each parameter that characterize the aerosol is difficult. Also, detailed modeling of droplet nucleation implies a high computational cost. Thus, sensitivity studies intend to determine whether the variability of some characteristics of the aerosol population can be neglected without introducing significant errors in the description of clouds.

A major debate refers to the relative importance of aerosol composition against size distribution and total number concentration (McFiggans et al., 2006). Several studies suggest that accurate measures of aerosol size and number concentration are more



important to obtain a relatively accurate description of cloud droplet populations (Feingold, 2003; Dusek et al., 2006; Ervens et al., 2007; Gunthe et al., 2009; Rose et al., 2010; Reutter et al., 2009). However, other observations/simulations show that, under certain circumstances, neglecting the variability of the aerosol composition prevent realistic estimations of the aerosol effect on clouds (Hudson, 2007; Quinn et al., 2008; Cubison et al., 2008; Roesler and Penner, 2010; Sánchez Gácita et al., 2017). This circumstantial sensitivity is commonly found in the literature and it refers not only to aerosol composition, but also to other meteorological/aerosol conditions (McFiggans et al., 2006). For instance, Feingold (2003) showed that the influence of aerosol parameters over the droplet effective radius ( $r_e$ ) varies as a function of aerosol loading. Under clean condition,  $r_e$  is mostly determined by the liquid water content and the aerosol number concentration ( $N_a$ ), with decreasing dependence on the aerosol size distribution, aerosol composition and vertical velocity ( $w$ ). However, under polluted conditions, all of them contribute significantly to  $r_e$ . Reutter et al. (2009) obtained that the variability of the initial cloud droplet number concentration ( $N_d$ ) in convective clouds is mostly dominated by the variability of  $w$  and  $N_a$ . They found that the hygroscopicity parameter ( $\kappa$ ) appears to play important roles at very low supersaturations in the updraft-limited regime of CCN activation. Also, a significant sensitivity of  $N_d$  on the aerosol size distribution parameters was found for some situations belonging to each one of the  $w - N_a$  regimes. Karydis et al. (2012) used a global meteorological model to obtain the sensitivity field of  $N_d$  to  $w$ , uptake coefficient,  $\kappa$  and  $N_a$ . They state that, overall,  $N_d$  is predicted to be less sensitive to changes in  $\kappa$  than in  $N_a$ , although there are regions and times where they result in comparable sensitivities.

To further evidence the importance of aerosol composition on clouds, Ward et al. (2010) consider the Reutter et al. (2009) environmental regimes but vary the log-normal median aerosol radius ( $\bar{r}_a$ ) to examine the behavior of the sensitivity to  $\kappa$ . Their results compare well with the Reutter et al. (2009) regime designation when using the same value of  $\bar{r}_a$ . However, they show that  $w/N_a$ , or supersaturation-based regimes, cannot fully predict the compositional dependence of CCN activity, it also varies significantly as a function of  $\bar{r}_a$ . It is remarkable that for small aerosols ( $\bar{r}_a < 0.06 \mu m$ ), composition affects CCN activity even in the aerosol-limited regime.

Most of the previous studies are based on the information from cloud-base. However, given the possibility of occurrence of cloud-top nucleation (Sun et al., 2012), it would be useful to assess the evolution of the cloud-top droplet size distribution (DSD), along with the cloud-base DSD, for exploring the aerosol first indirect effect. In a growing cumulus, the cloud-top represents the beginning of the cloud development at each level, including cloud-base –because, in the initial stage of the cloud life-cycle, both the base and the top coincide in space. Thus, the characteristics of the DSD at cloud-top will strongly impact the evolution of the cloud, modulating the rates of microphysical process onward and therefore determining the structure of the cloud. As Cecchini et al. (2017) pointed out, studies should take into account the altitude above cloud base. The authors showed that, on average, droplet growth with cloud evolution is comparable in absolute value and is opposite to the aerosol effect. They determined that the aerosol effect on DSD shape inverts in sign with altitude, favoring broader droplet distributions close to cloud base but narrower DSDs higher in the clouds.

With ample water vapor supply, high temperatures and a wide spectrum of aerosol conditions, the troposphere over the Amazon constitutes an ideal scenario to study aerosol-cloud-precipitation interaction. Because they belong to the “aerosol-limited regime”, characterized by strong updrafts and a low aerosol background concentration (Reutter et al., 2009), Amazonian



clouds are found to be very sensitive to aerosols (Andreae et al., 2004; Braga et al., 2017; Cecchini et al., 2017; Fan et al., 2018; Reid et al., 1999). At the same time, clouds control both the removal and production of atmospheric particles over the Amazon basin. According to Andreae et al. (2018), the production of new aerosol particles from biogenic volatile organic material, brought up by deep convection to the upper troposphere, is the dominant process supplying secondary aerosol particles in the pristine atmosphere. Then, those particles can be transported from the free troposphere into the boundary layer by strong convective downdrafts or even weaker downward motions in the trailing stratiform region of convective systems (Wang et al., 2016).

Here we propose to explore the cloud sensitivities to several aerosol properties, by simulating some characteristics of Amazon clouds. We focus on the information from cloud-top, during the warm stages of cloud life-cycle, using a sample strategy that also includes the information from the cloud-base at the initial stage of development of the cloud. Our approach is similar to Ward et al. (2010), but it is not limited to analyze the hygroscopicity sensitivity. Instead, we extended the discussion to the sensitivity to the aerosol median size and number concentration too, and consider their effects on both droplet size and concentration.

## 2 Modelling approach

The model employed here consists of a bin microphysics parameterization (Feingold et al., 1988; Tzivion et al., 1987, 1989) coupled to a single-column Eulerian framework, the Kinematic Driver (KiD) (Shipway and Hill, 2012), with prescribed  $w$ . Thus, at each time step, every grid-point parcel receives an influence from two sources: advection and microphysics processes.

The KiD prognostic variables are potential temperature (K) and water vapor, hydrometeor and aerosol mixing ratios ( $\text{kg kg}^{-1}$ ). It uses the Exner pressure as a fixed vertical coordinate and the total variance-diminishing scheme (Leonard et al., 1993) as the default advection scheme. Its prognostic variables are held on “full” model levels, while  $w$  and the density are held on both “full” and “half” levels such that the grid can be used as a Lorenz-type (Lorenz, 1960) or Charney-Phillips-type (Charney and Phillips, 1953) grid.

The KiD model was conceived as a kinematic framework to compare different microphysics parameterizations without addressing the microphysics-dynamics feedbacks. Thus, obtaining precise quantitative simulations with KiD cannot be expected; nevertheless, it can provide important insights about the responses of the simulated cloud to changes in the parameters of the microphysics scheme.

In our simulations, a 1 s time step was used for both dynamics and microphysics algorithms during an integration time of 1200 s (20 min). For the vertical domain, a 120-level grid was defined with a 50-m grid spacing from 0 m to 6000 m of altitude.

As initial conditions, vertical profiles of potential temperature and water vapor mixing ratio from an in situ atmospheric sounding<sup>1</sup> were provided (Fig. 1a). We used the 12Z sounding, on September 11, 2014, from Boa Vista-RR, Brazil. The sounding data were interpolated to match the model resolution and then smoothed to represent a more general situation.

<sup>1</sup><http://weather.uwyo.edu/upperair/sounding.html>



Here, the vertical velocity field ( $w(z, t)$ ) was constructed based on the idea of having a layer of positive buoyancy, where a parcel updraft velocity would increase with height until reaching the negative buoyancy layer. The defined time dependence for the velocity maximum and its height roughly simulate the acceleration that the air must experience and the progressive destabilization of the air column (Fig. 1b).

$$w(z, t) = \begin{cases} W \sin\left(\frac{\pi}{2} \frac{t}{T}\right) e^{-\frac{1}{2} \log^2(0.004t - 0.0008z)} & (0.2z - t) < 0 \\ 0 & \text{otherwise} \end{cases} \quad (1)$$

In Eq. 1,  $W$  represents the maximum updraft speed (with respect to both height and time) in  $\text{m s}^{-1}$  and  $T$  is the length of the simulation in s. The value of  $W$  was set to  $5 \text{ m s}^{-1}$  taking into account the measurements of the ACRIDICON-CHUVA AC09 flight, where the  $w$  oscillated between  $0 \text{ m s}^{-1}$  and  $8 \text{ m s}^{-1}$  (Cecchini et al., 2017). This flight was performed by the High Altitude and Long Range Research Aircraft (HALO) on the same date of the aforementioned sounding (Wendisch et al., 2016; Machado et al., 2014). It sampled the top of growing convective cumulus over remote regions of the Amazon, starting close to the local noon, in the dry-to-wet season transition.

## 2.1 Microphysics representation

For the simulations performed in this work, we have used the TAU<sup>2</sup> size-bin-resolved microphysics scheme that was first developed by Tzivion et al. (1987, 1989) and Feingold et al. (1988) with later applications and development documented in Stevens et al. (1996); Reisn et al. (1998); Yin et al. (2000b, a) and Rotach and Zardi (2007).

TAU differs from other bin microphysical codes because it solves for two moments of the drop size distribution in each of the bins rather than solving the equations for the explicit size distribution at each mass/size point, which allows for a more accurate transfer of mass between bins and alleviates anomalous drop growth.

In this version of the TAU microphysics<sup>3</sup>, the cloud drop size distribution is divided into 34 mass-doubling bins with radii ranging between  $1.56 \mu\text{m}$  and  $3200 \mu\text{m}$ . The method of moments (Tzivion et al., 1987) is used to compute mass and number concentrations in each size bin resulting from diffusional growth (Tzivion et al., 1989), collision-coalescence and collisional breakup (Tzivion et al., 1987; Feingold et al., 1988). Sedimentation is performed with a first-order upwind scheme. Aerosols are represented by a single prognostic variable, its bulk number concentration, which is assumed to follow a log-normal size distribution. Thus, activation is calculated by applying Köhler's theory to this aerosol distribution, using a 0.25 factor that attempts to accommodate for the fact that not all CCN will grow to the size of the first bin of the droplet distribution.

One disadvantage of our approach is the lack of an explicit representation of the droplet activation mechanism, that would require the definition of bins to simulate the hygroscopic growth of aerosol particles. Another source of inaccuracies comes from considering only one aerosol mode with a single value of  $\kappa$ , ignoring quasi-internal or external mixing states (Rissman et al., 2004; McFiggans et al., 2006; Ervens et al., 2007). However, at first, this approach makes our results suitable to understand how changes in the aerosol properties affect the simulations of numerical models in operational or research configurations, which rarely use a detailed description of the aerosols.

<sup>2</sup>The acronym TAU refers to the Tel Aviv University, where it was primarily developed

<sup>3</sup>Version available at <https://www.esrl.noaa.gov/csd/staff/graham.feingold/code/> (Accessed on: 04/11/2017)



### 3 Sensitivity analysis

We employ a phase space defined by two bulk properties of the DSD (hereinafter “bulk phase space”):  $N_d$  ( $\text{cm}^{-3}$ ), which coincides with the zeroth moment of the DSD, and  $D_{eff}$  ( $\mu\text{m}$ ), which is the ratio between the third and second moments.

Sensitivity tests in the bulk phase space provide a very efficient means to evaluate how a specific parameter variability can affect the evolution of cloud-top DSDs. Here, we test the sensitivity of  $N_d$  and  $D_{eff}$  at the cloud top to variations in  $N_a$ ,  $\bar{r}_a$ , the geometric standard deviation ( $\sigma_a$ ) of the aerosol size distribution and  $\kappa$ , using ranges normally found in the Amazon atmosphere (Gunthe et al., 2009; Martin et al., 2010; Pöhlker et al., 2016) (Table 1).

**Table 1.** Aerosol parameters used for the sensitivity tests: intervals for values and steps between them.

Parameter	Interval	Step
$N_a$ ( $\text{cm}^{-3}$ )	200 – 900	100
$\bar{r}_a$ ( $\mu\text{m}$ )	0.02 – 0.08	0.01
$\sigma_a$ ()	1.1 – 1.9	0.2
$\kappa$ ()	0.1 – 0.5	0.1

The sensitivities were calculated as the slope of the linear fit between  $Y$  and  $X_i$  in logarithmic scale for normalization:

$$S_Y(X_i) = \left. \frac{\partial \ln Y}{\partial \ln X_i} \right|_{X_k} \quad (2)$$

where  $Y$  represents either  $N_d$  or  $D_{eff}$ , and  $X_i$  is the aerosol property affecting  $Y$ .  $S_Y(X_i)$  represents the relative change in  $Y$  for a relative change in  $X_i$  and places less reliance on the absolute measures of parameters (Feingold, 2003; Reutter et al., 2009; Ward et al., 2010). The subscript  $X_k$  indicates that when calculating the sensitivity to  $X_i$ , the other aerosol parameters are held constant. For each value at which  $X_k$  is fixed, we will obtain a new value of  $S_Y(X_i)$ , i.e. we can also calculate  $S_Y(X_i)$  as a function of  $X_k$  ( $S_Y(X_i, X_k)$ ).

The latter differentiates our approach from previous studies. Feingold (2003) included the variability of all  $X \neq X_i$  when calculating the linear regression between  $\ln Y$  and  $\ln X_i$ , only distinguishing the results for two subsets of  $N_a$ . Similarly, Reutter et al. (2009) analyzed the sensitivities to  $\bar{r}_a$ ,  $\sigma_a$  and  $\kappa$  for three combinations of  $N_a$  and  $w$ , but all values of  $Y$  calculated at a given value of  $X_i$  were averaged prior to fitting. This analysis was then expanded by Ward et al. (2010), who calculated  $S_{N_d}(\kappa)$  for different values of  $\bar{r}_a$  and  $\sigma_a$  used to initialize the parcel model. Now, we use a more general approach that allows us to study the responses of both cloud droplet number concentration and effective diameter to changes in each aerosol characteristic, as a function of the other aerosol parameters used to initialize the model.



## 4 Results

The cloud-top was defined here as the last model level, from surface to top, where the droplet concentration was larger than 100 per  $\text{cm}^3$ . It is represented by black lines in Fig. 2. Figure 2 shows  $N_d$ ,  $D_{eff}$  and the mixing ratio of cloud droplets ( $q_c$ ), for the entire simulation. Note that the upward advection causes a maximum of  $N_d$  at cloud-top for all times. As droplets ascend and mix with new droplets, they grow by diffusion of vapor and, to a lesser extent, by collision-coalescence. As a consequence,  $D_{eff}$  and  $q_c$  are larger in upper levels at the last times of the simulation.

Firstly, we represented the cloud-top information in the bulk phase space to discuss the “isolated” effect of each parameter, when fixing the values of the others. The control values of the parameters employed here are  $N_a=800\text{cm}^{-3}$ ,  $\bar{r}_a=0.05\mu\text{m}$ ,  $\sigma_a=1.5$ , and  $\kappa=0.1$ .

Figure 3a shows the sensitivity of cloud-top DSDs to the initial concentration of aerosols. Note that an increase of the aerosol concentration increases the number of activated drops, as expected. This nucleation enhancement induces a smaller effective diameter because of water vapor competition, despite a slightly increased liquid water content (not shown). Thus, if the water vapor amount is kept constant, the diffusional growth for each droplet is slowed. The latter manifests as a trend to the horizontal orientation (in the direction of larger values of  $N_d$ ) in the bulk phase space. For the most polluted situations, a tendency to attain an almost constant effective diameter is evidenced.

Figure 3b shows the sensitivity of cloud-top DSDs to the median radius of the aerosol population. The effects of increasing  $\bar{r}_a$  are similar to the consequences of increasing  $N_a$ . If we keep the aerosol size distribution shape constant (i.e. the same total concentration and standard deviation) and increase  $\bar{r}_a$ , then more droplets are activated because of the larger availability of aerosols with sizes above the activation threshold. Thus, nucleation increases, whereas diffusional growth decreases.

The tests in Fig. 3 evidence a type of “saturation” effect for the larger values of  $\bar{r}_a$  tested, i.e. the sensitivity decreases as this parameter increases. The combination of two factors explains this behavior: the water vapor availability and the position of the size distribution curve with respect to the critical radius for droplet activation ( $r_c$ ). Even if continuous water vapor supply from the surface occurs, the water vapor can be completely consumed in each time step, depending on the aerosol availability and the diffusional growth rate. If the number of activated aerosols is able to consume all the water vapor that reaches a layer in a time step, an increase of its quantity will not introduce differences in the DSD. Moreover, for certain positions of the size distribution curve with respect to  $r_c$ , an increment in  $\bar{r}_a$  does not produce a significant impact on the number of activated aerosols.

Figure 3c shows the sensitivity to the standard deviation of the aerosol size distribution. In our tests, increasing this parameter also causes an increment of the droplet concentration through an enhancement of the nucleation rate. However, the effect of varying  $\sigma_a$  is more important at the earliest stages/lowest levels of the cloud (the extremity with the smallest values of  $N_d$  and effective diameter in each path).  $\sigma_a$  modifies the shape of the aerosol size distribution. Although an increase of  $\bar{r}_a$  always enhances the number of activated droplets, the same does not apply to  $\sigma_a$ . Instead, the effects of changing  $\sigma_a$  depend on the position of  $r_c$  with respect to the size distribution function. For certain values of  $r_c$ , increasing  $\sigma_a$  can induce a reduction in the number of droplets that become activated, whereas, for others, it can cause an increase of the number of activated droplets



(non-monotonic behavior). Given that  $r_c$  varies with height, it explains the differences in the effect of  $\sigma_a$  as the cloud height increases. These tests also illustrate that the sensitivity is larger for smaller values of  $\sigma_a$ , because the log-normal distribution shape is more sensitive to  $\sigma_a$  in the interval 1.1-1.5 than in 1.5-1.9.

Finally, Fig. 3d shows the effects of varying  $\kappa$  in the simulation. Given the control values of the other parameters, the effect of changing  $\kappa$  is relatively small. Nevertheless, we can see that increasing  $\kappa$  favors the nucleation through a decrease of  $r_c$ . As a consequence,  $N_d$  increases, whereas the effective diameter decreases.

The previously mentioned saturation effect can be identified for every spectrum of tests in Fig. 3. There is always an interval of values of the tested parameter in which the system becomes less sensitive. The latter has been discussed before in the literature; for example, it is known that the sensitivity to  $\kappa$  increases substantially as  $\kappa$  decreases (Petters and Kreidenweis, 2007). However, that effect is more or less evident depending on the values of the other parameters.

To illustrate that sensitivity variation, we calculated  $S_{\bar{N}_d}(X_i)$  and  $S_{\bar{D}_{eff}}(X_i)$ , with  $X_i$  being  $N_a$ ,  $\bar{r}_a$ ,  $\sigma_a$  or  $\kappa$ .  $\bar{N}_d$  and  $\bar{D}_{eff}$  are the time averages of  $N_d$  and  $D_{eff}$  at cloud-top for each simulation, respectively. From Eq. 2,  $S_{\bar{N}_d}(N_a)$ , for example, is the slope of the linear fit between the values of  $\bar{N}_d$  and  $N_a$  in logarithmic scale, for a given combination of  $\bar{r}_a$ ,  $\sigma_a$  and  $\kappa$ . The sensitivity to one aerosol parameter can then be calculated a number of times equivalent to all possible combinations of the values of the other parameters in Table 1. From its definition, it follows that positive (negative) values of  $S_Y(X_i)$  correspond to increasing (decreasing)  $Y$  as  $X_i$  increases. Also,  $|S_Y(X_i)| = 1$  means that a given variation in  $X_i$  is accompanied by the same absolute variation in  $Y$ .

Figures 4, 5, 6 and 7 show  $S_Y(X_i)$  as a function of all values of  $N_a$ ,  $\bar{r}_a$ ,  $\sigma_a$  and  $\kappa$  considered. Generally,  $\bar{N}_d$  can be almost three times more sensitive to changes in the aerosol parameters than  $\bar{D}_{eff}$ , which stems from the mathematical definition of these physical magnitudes. Also, the results for  $S_Y(N_a)$  agree with the theoretical limits referred in the literature and all sensitivity calculations include the ranges of previously reported values (Feingold, 2003; Reutter et al., 2009; Ward et al., 2010). For each value in the x-axis of figures 4, 5, 6 and 7, there are several combinations of the other two parameters; as a result, there are several points for each value of the x-axis in the figures.

The impact of  $N_a$  on cloud droplets depends on the values of  $\bar{r}_a$ ,  $\sigma_a$  and  $\kappa$ , as can be seen in Fig. 4. However, this dependency is stronger for the parameters that define the aerosol size distribution,  $\bar{r}_a$  and  $\sigma_a$ , than for  $\kappa$ . Note that in Fig. 4c, varying  $\kappa$  has a small effect on the distribution of the points, compared to the effects of varying  $\bar{r}_a$  and  $\sigma_a$  in Figs. 4a and 4b, respectively. The points are more dispersed for smaller  $\bar{r}_a$  and  $\sigma_a$  and tend to be concentrated around a maximum sensitivity value as  $\bar{r}_a$  increases. Generally, for smaller values of  $\bar{r}_a$ ,  $\sigma_a$  and  $\kappa$ ,  $S_Y(N_a)$  can be almost null, i.e. no more or less droplets are being formed, nor its size distribution is being modified, regardless of the quantity of aerosol in the environment. In the vicinity of this state, the activation of droplets is being determined by the characteristics of the aerosol, instead of its number concentration. Hence, for smaller aerosols, the relative importance of the aerosol properties can be opposite to that at larger sizes. To complement the previous analysis, Figures 6b and 7c evidence that the sensitivity to  $\sigma_a$  and  $\kappa$ , respectively, can be significantly increased for smaller values of  $\bar{r}_a$ .

Figure 5a shows that the sensitivity to the median radius of the aerosol population increases for higher values of  $N_a$ —which agrees with Feingold (2003) and Rissman et al. (2004)—and for lower values of  $\sigma_a$  and  $\kappa$ . Interestingly, the lower variability



in  $S_Y(\bar{r}_a)$  corresponds to the values of  $N_a$ ,  $\sigma_a$  and  $\kappa$  where the absolute value of the mean sensitivity is minimum, which is opposite to the behavior of  $S_Y(N_a)$ .

The same applies to the sensitivity to the geometric standard deviation of the aerosol size distribution (Fig. 6), substituting  $\sigma_a$  by  $\bar{r}_a$  as the independent variable in Fig. 6b. However, it is remarkable that the absolute values of  $S_Y(\sigma_a)$  are the highest between those analyzed here. Thus, the width of the aerosol spectrum can be more important for droplet activation than the aerosol median radius, total concentration and composition. The reason for the small sensitivity evidenced in fig. 3c is the value of  $\bar{r}_a$  taken as a reference there. Nevertheless, it is important to remember that, even having a high potential impact (determined by the value of  $S_Y(\sigma_a)$  in this case), the effect of varying a parameter will be determined by its range of possible values. For example, assuming that the maximum and minimum values specified in Table 1 determine the entire variation of the parameters in a given situation, it follows that the modification of the DSD induced by a variation of 0.8 in  $\sigma_a$  (an increase ratio of 1.72) would be smaller than the changes in droplet size and number concentration due to a 0.06- $\mu\text{m}$  variation in  $\bar{r}_a$  (an increase ratio of 4).

Note that  $S_Y(\sigma_a)$  changes its sign, which is related to the previously commented variations in the effect of  $\sigma_a$  depending on the position of  $r_c$  with respect to the size distribution function. The positive values obtained by Feingold (2003) for the sensitivity of droplet size on  $\sigma_a$ , as well as the negative values reported by Reutter et al. (2009) for the sensitivity of droplet number concentration on  $\sigma_a$  should be due to the inclusion of larger aerosol sizes, where those signs are predominant (see Fig. 6b).

The effects of  $\kappa$  on the sensitivity to size parameters is higher compared to its effect on  $S_Y(N_a)$ , i.e. the composition of the aerosol can significantly affect the way droplets respond to changes in the aerosol size distribution (Figs. 5c and 6c).

Finally, the sensitivity to the aerosol hygroscopicity is the lowest between those analyzed here (Fig. 7). The absolute value of  $S_Y(\kappa)$  is larger for higher  $N_a$  and smaller  $\bar{r}_a$  and  $\sigma_a$ , and has a small dependency on  $N_a$ , for most of the values considered here. Note that, for the intervals of  $N_a$ ,  $\bar{r}_a$  and  $\sigma_a$  where the absolute value of  $S_Y(\kappa)$  is maximum, it is still smaller than the sensitivity to those parameters in the same interval. However, its influence can be more than 50% of the sensitivity to  $N_a$ , which confirms that neglecting the effects of the aerosol composition is non trivial. Moreover, the effects of the aerosol composition can be significantly increased in conditions of weak updrafts (Ervens et al., 2005; Anttila and Kerminen, 2007; Reutter et al., 2009). That, in combination with the values of  $N_a$ ,  $\bar{r}_a$  and  $\sigma_a$  can determine an even more important role for  $\kappa$ . As Ward et al. (2010) concluded, the influence of variations in the shape parameter on  $S_Y(\kappa)$  are more important for small  $\bar{r}_a$ . This is evidenced by the dispersion of the points for  $\bar{r}_a < 0.05\mu\text{m}$  in Fig. 7b. Of course, that dispersion includes the responses to changes in  $N_a$  too, it is not entirely caused by the  $\sigma_a$  variability. The information contained in Fig. 7b agrees with the sensitivity of droplets to changes in  $\kappa$ , computed by Ward et al. (2010) for the aerosol-limited regime, as a function of  $\bar{r}_a$ .

From our analysis it turns out that  $\bar{r}_a$  is the most important parameter, from those analyzed, that influences the sensitivity to aerosols. This is particularly interesting because of the importance that has been conventionally attributed to the aerosol number concentration. Considering this sensitivity limitation, for certain conditions, other variables, such as the aerosol median size and size distribution shape, can be more influential in determining the evolution of an air parcel.





We calculated the time-averaged values of  $N_d$  and  $D_{eff}$  for the cloud-top DSDs at each simulation. Figure 8 shows the mean and standard deviation of these averages for each value of  $N_a$  tested. The length of the standard deviation bars is determined by the ranges of  $\bar{r}_a$ ,  $\sigma_a$  and  $\kappa$ . Figure 8a represents the generally accepted knowledge: given a certain temperature and water vapor availability, the bulk properties of a cloud are mostly determined by  $N_a$ . However, this behavior seems to be valid only for the largest values of  $\bar{r}_a$ . If the aerosol size distribution is displaced to a smaller radius (Figure 8b), then more aerosol characteristics must be specified.

Our results show that the study of the aerosol-cloud interaction must include the parameters describing aerosol properties, such as the size and hygroscopicity, at least for  $\bar{r}_a \leq 0.05 \mu\text{m}$ . These parameters can produce changes in the DSD as large as those caused by changes in the aerosol concentration. The error associated with its misrepresentation increases with aerosol loading and can be as large as 23% in  $N_d$  and 15% in  $D_{eff}$  for  $N_a = 800 \text{ cm}^{-3}$ , which is larger than the error introduced by a 25% variation in  $N_a$ , according to Fig. 8b. Note that aerosol loads larger than  $800 \text{ cm}^{-3}$  are common in the Amazon, due to biomass burning. These findings are also relevant given the current discussion about the importance of ultrafine aerosol particles in the development of deep convective clouds over the Amazon (Wang et al., 2016; Fan et al., 2018).

## 5 Summary and conclusions

We illustrated the influence of the aerosol number concentration, the median radius and geometric standard deviation of the aerosol size distribution, and the hygroscopicity of the aerosols on the number concentration and effective diameter of droplets at the top of warm-phase clouds, for initial conditions typical of the Amazon. Given the tested variations in the aerosol properties, the cloud DSDs were found to behave as expected. Overall, when the nucleation is favored, an increase in the droplet number concentration is accompanied by a decrease in the droplet effective diameter. The effects of the investigated parameters were similar in all stages of the cloud-top evolution, except for the geometric standard deviation of the aerosol size distribution. Changes in the aerosol size distribution shape were more important in the earliest stages of the cloud –lower cloud-top heights– due to its dependence on the position of  $r_c$  with respect to the size distribution function.

We showed that the sensitivity to each aerosol characteristic varies as a function of the tested parameter and its value depends on the base value of the other parameters. The median radius of the aerosols is the most important parameter, from those analyzed, that influences the sensitivity to the others. Based on its value, it is possible to define, inside Reutter et al. (2009) aerosol limited-regime, a concentration-limited regime, when other aerosol properties can be neglected, and a regime where all size distribution characteristics, total number concentration and hygroscopicity significantly influences the droplet number concentration and effective diameter. This expands the result of Ward et al. (2010) and states that  $w/N_a$ , or supersaturation-based regimes (Reutter et al., 2009), cannot fully predict the dependence of CCN activity, not only on the aerosol composition, but on all aerosol characteristics.

Despite using a simpler modeling approach, our results agree with previous studies, which assures the validity of our calculations. Thus, the application of these conclusions is not limited to models that use a similar representation of microphysics processes, but also to theoretical or experimental studies.



*Author contributions.* LHP performed the model simulations, the model–data analysis and prepared the manuscript. LATM and MAC provided guidance with the definition of the model initial conditions. LATM, MAC and MSG provided guidance with the choice of the variables and its interval of values and the model–data analysis. All authors contributed to the design of the study and the preparation of the manuscript.

*Competing interests.* The authors declare that they have no conflict of interest.

- 5 *Acknowledgements.* This research was funded by the SOS CHUVA FAPESP Project 2015/14497-0. The contributions of Micael A. Cecchini and Lianet H. Pardo were funded by FAPESP grants 2017/04654-6 and 2016/24562-6, respectively.



## References

- Albrecht, B. A.: Aerosols, Cloud Microphysics, and Fractional Cloudiness, *Science*, 245, 1227–1230, <https://doi.org/10.1126/science.245.4923.1227>, 1989.
- Andreae, M. O., Rosenfeld, D., Artaxo, P., Costa, A. A., Frank, G. P., Longo, K. M., and Silva-Dias, M. A. F.: Smoking Rain Clouds over the Amazon, *Science*, 303, 1337–1342, <https://doi.org/10.1126/science.1092779>, 2004.
- Andreae, M. O., Afchine, A., Albrecht, R., Holanda, B. A., Artaxo, P., Barbosa, H. M. J., Borrmann, S., Cecchini, M. A., Costa, A., Dollner, M., Fütterer, D., Järvinen, E., Jurkat, T., Klimach, T., Konemann, T., Knote, C., Krämer, M., Krisna, T., Machado, L. A. T., Mertes, S., Minikin, A., Pöhlker, C., Pöhlker, M. L., Pöschl, U., Rosenfeld, D., Sauer, D., Schlager, H., Schnaiter, M., Schneider, J., Schulz, C., Spanu, A., Sperling, V. B., Voigt, C., Walser, A., Wang, J., Weinzierl, B., Wendisch, M., and Ziereis, H.: Aerosol characteristics and particle production in the upper troposphere over the Amazon Basin, *Atmospheric Chemistry and Physics*, 18, 921–961, <https://doi.org/10.5194/acp-18-921-2018>, 2018.
- Anttila, T. and Kerminen, V.-M.: On the contribution of Aitken mode particles to cloud droplet populations at continental background areas – a parametric sensitivity study, *Atmospheric Chemistry and Physics*, 7, 4625–4637, <https://doi.org/10.5194/acp-7-4625-2007>, 2007.
- Braga, R. C., Rosenfeld, D., Weigel, R., Jurkat, T., Andreae, M. O., Wendisch, M., Pöschl, U., Voigt, C., Mahnke, C., Borrmann, S., Albrecht, R. I., Molleker, S., Vila, D. A., Machado, L. A. T., and Grulich, L.: Further evidence for CCN aerosol concentrations determining the height of warm rain and ice initiation in convective clouds over the Amazon basin, *Atmospheric Chemistry and Physics*, 17, 14 433–14 456, <https://doi.org/10.5194/acp-17-14433-2017>, 2017.
- Cecchini, M. A., Machado, L. A. T., Andreae, M. O., Martin, S. T., Albrecht, R. I., Artaxo, P., Barbosa, H. M. J., Borrmann, S., Fütterer, D., Jurkat, T., Mahnke, C., Minikin, A., Molleker, S., Pöhlker, M. L., Pöschl, U., Rosenfeld, D., Voigt, C., Weinzierl, B., and Wendisch, M.: Sensitivities of Amazonian clouds to aerosols and updraft speed, *Atmospheric Chemistry and Physics*, 17, 10 037–10 050, <https://doi.org/10.5194/acp-17-10037-2017>, 2017.
- Charney, J. G. and Phillips, N. A.: Numerical integration of the quasi-geostrophic equations for barotropic and simple baroclinic flows, *Journal of Meteorology*, 10, 71–99, [https://doi.org/10.1175/1520-0469\(1953\)010<0071:NIOTQG>2.0.CO;2](https://doi.org/10.1175/1520-0469(1953)010<0071:NIOTQG>2.0.CO;2), 1953.
- Cubison, M. J., Ervens, B., Feingold, G., Docherty, K. S., Ulbrich, I. M., Shields, L., Prather, K., Hering, S., and Jimenez, J. L.: The influence of chemical composition and mixing state of Los Angeles urban aerosol on CCN number and cloud properties, *Atmospheric Chemistry and Physics*, 8, 5649–5667, <https://doi.org/10.5194/acp-8-5649-2008>, 2008.
- Dusek, U., Frank, G. P., Hildebrandt, L., Curtius, J., Schneider, J., Walter, S., Chand, D., Drewnick, F., Hings, S., Jung, D., Borrmann, S., and Andreae, M. O.: Size Matters More Than Chemistry for Cloud-Nucleating Ability of Aerosol Particles, *Science*, 312, 1375–1378, <https://doi.org/10.1126/science.1125261>, 2006.
- Ervens, B., Feingold, G., and Kreidenweis, S. M.: Influence of water-soluble organic carbon on cloud drop number concentration, *Journal of Geophysical Research: Atmospheres*, 110, <https://doi.org/10.1029/2004JD005634>, 2005.
- Ervens, B., Cubison, M., Andrews, E., Feingold, G., Ogren, J. A., Jimenez, J. L., DeCarlo, P., and Nenes, A.: Prediction of cloud condensation nucleus number concentration using measurements of aerosol size distributions and composition and light scattering enhancement due to humidity, *Journal of Geophysical Research: Atmospheres*, 112, <https://doi.org/10.1029/2006JD007426>, 2007.
- Fan, J., Zhang, R., Li, G., Tao, W.-K., and Li, X.: Simulations of cumulus clouds using a spectral microphysics cloud-resolving model, *Journal of Geophysical Research: Atmospheres*, 112, <https://doi.org/10.1029/2006JD007688>, 2007.



- Fan, J., Rosenfeld, D., Zhang, Y., Giangrande, S. E., Li, Z., Machado, L. A. T., Martin, S. T., Yang, Y., Wang, J., Artaxo, P., Barbosa, H. M. J., Braga, R. C., Comstock, J. M., Feng, Z., Gao, W., Gomes, H. B., Mei, F., Pöhlker, C., Pöhlker, M. L., Pöschl, U., and de Souza, R. A. F.: Substantial convection and precipitation enhancements by ultrafine aerosol particles, *Science*, 359, 411–418, <https://doi.org/10.1126/science.aan8461>, 2018.
- 5 Feingold, G.: Modeling of the first indirect effect: Analysis of measurement requirements, *Geophysical Research Letters*, 30, <https://doi.org/10.1029/2003GL017967>, 2003.
- Feingold, G., Tzivion, S., and Leviv, Z.: Evolution of Raindrop Spectra. Part I: Solution to the Stochastic Collection/Breakup Equation Using the Method of Moments, *Journal of the Atmospheric Sciences*, 45, 3387–3399, [https://doi.org/10.1175/1520-0469\(1988\)045<3387:EORSPI>2.0.CO;2](https://doi.org/10.1175/1520-0469(1988)045<3387:EORSPI>2.0.CO;2), 1988.
- 10 Gonçalves, W. A., Machado, L. A. T., and Kirstetter, P.-E.: Influence of biomass aerosol on precipitation over the Central Amazon: an observational study, *Atmospheric Chemistry and Physics*, 15, 6789–6800, <https://doi.org/10.5194/acp-15-6789-2015>, 2015.
- Gunthe, S. S., King, S. M., Rose, D., Chen, Q., Roldin, P., Farmer, D. K., Jimenez, J. L., Artaxo, P., Andreae, M. O., Martin, S. T., and Pöschl, U.: Cloud condensation nuclei in pristine tropical rainforest air of Amazonia: size-resolved measurements and modeling of atmospheric aerosol composition and CCN activity, *Atmospheric Chemistry and Physics*, 9, 7551–7575, <https://doi.org/10.5194/acp-9-7551-2009>,  
15 2009.
- Heiblum, R. H., Altaratz, O., Koren, I., Feingold, G., Kostinski, A. B., Khain, A. P., Ovchinnikov, M., Fredj, E., Dagan, G., Pinto, L., Yaish, R., and Chen, Q.: Characterization of cumulus cloud fields using trajectories in the center of gravity versus water mass phase space: 2. Aerosol effects on warm convective clouds, *Journal of Geophysical Research: Atmospheres*, 121, 6356–6373, <https://doi.org/10.1002/2015JD024193>, 2016.
- 20 Hudson, J. G.: Variability of the relationship between particle size and cloud-nucleating ability, *Geophysical Research Letters*, 34, <https://doi.org/10.1029/2006GL028850>, 2007.
- Karydis, V. A., Capps, S. L., Russell, A. G., and Nenes, A.: Adjoint sensitivity of global cloud droplet number to aerosol and dynamical parameters, *Atmospheric Chemistry and Physics*, 12, 9041–9055, <https://doi.org/10.5194/acp-12-9041-2012>, 2012.
- Khain, A., Rosenfeld, D., and Pokrovsky, A.: Aerosol impact on the dynamics and microphysics of deep convective clouds, *Quarterly Journal of the Royal Meteorological Society*, 131, 2639–2663, <https://doi.org/10.1256/qj.04.62>, 2005.
- 25 Koren, I., Feingold, G., and Remer, L. A.: The invigoration of deep convective clouds over the Atlantic: aerosol effect, meteorology or retrieval artifact?, *Atmospheric Chemistry and Physics*, 10, 8855–8872, <https://doi.org/10.5194/acp-10-8855-2010>, 2010.
- Lee, S. S., Donner, L. J., Phillips, V. T. J., and Ming, Y.: Examination of aerosol effects on precipitation in deep convective clouds during the 1997 ARM summer experiment, *Quarterly Journal of the Royal Meteorological Society*, 134, 1201–1220, <https://doi.org/10.1002/qj.287>,  
30 2008.
- Leonard, B., MacVean, M., and Lock, A.: Positivity-preserving numerical schemes for multidimensional advection, Technical Report, NASA, United States, 64 pp., 1993.
- Li, Z., Niu, F., Fan, J., Liu, Y., Rosenfeld, D., and Ding, Y.: Long-term impacts of aerosols on the vertical development of clouds and precipitation, *Nature Geoscience*, 4, 888–894, <https://doi.org/10.1038/NGEO1313>, 2011.
- 35 Lorenz, E. N.: Energy and Numerical Weather Prediction, *Tellus*, 12, 364–373, <https://doi.org/10.3402/tellusa.v12i4.9420>, 1960.
- Machado, L. A. T., Silva Dias, M. A. F., Morales, C., Fisch, G., Vila, D., Albrecht, R., Goodman, S. J., Calheiros, A. J. P., Biscaro, T., Kummerow, C., Cohen, J., Fitzjarrald, D., Nascimento, E. L., Sakamoto, M. S., Cunningham, C., Chaboureaud, J.-P., Petersen, W. A., Adams, D. K., Baldini, L., Angelis, C. F., Sapucci, L. F., Salio, P., Barbosa, H. M. J., Landulfo, E., Souza, R. A. F., Blakeslee, R. J.,



- Bailey, J., Freitas, S., Lima, W. F. A., and Tokay, A.: The Chuva Project: How Does Convection Vary across Brazil?, *Bulletin of the American Meteorological Society*, 95, 1365–1380, <https://doi.org/10.1175/BAMS-D-13-00084.1>, 2014.
- Martin, S. T., Andreae, M. O., Artaxo, P., Baumgardner, D., Chen, Q., Goldstein, A. H., Guenther, A., Heald, C. L., Mayol-Bracero, O. L., McMurphy, P. H., Pauliquevis, T., Pöschl, U., Prather, K. A., Roberts, G. C., Saleska, S. R., Silva Dias, M. A., Spracklen, D. V., Swietlicki, E., and Trebs, I.: Sources and properties of Amazonian aerosol particles, *Reviews of Geophysics*, 48, <https://doi.org/10.1029/2008RG000280>, 2010.
- McFiggans, G., Artaxo, P., Baltensperger, U., Coe, H., Facchini, M. C., Feingold, G., Fuzzi, S., Gysel, M., Laaksonen, A., Lohmann, U., Mentel, T. F., Murphy, D. M., O'Dowd, C. D., Snider, J. R., and Weingartner, E.: The effect of physical and chemical aerosol properties on warm cloud droplet activation, *Atmospheric Chemistry and Physics*, 6, 2593–2649, <https://doi.org/10.5194/acp-6-2593-2006>, 2006.
- 10 Petters, M. D. and Kreidenweis, S. M.: A single parameter representation of hygroscopic growth and cloud condensation nucleus activity, *Atmospheric Chemistry and Physics*, 7, 1961–1971, <https://doi.org/10.5194/acp-7-1961-2007>, 2007.
- Pöhlker, M. L., Pöhlker, C., Ditas, F., Klimach, T., Hrabec de Angelis, I., Araújo, A., Brito, J., Carbone, S., Cheng, Y., Chi, X., Ditz, R., Gunthe, S. S., Kesselmeier, J., Könemann, T., Lavrič, J. V., Martin, S. T., Mikhailov, E., Moran-Zuloaga, D., Rose, D., Saturno, J., Su, H., Thalman, R., Walter, D., Wang, J., Wolff, S., Barbosa, H. M. J., Artaxo, P., Andreae, M. O., and Pöschl, U.: Long-term observations of cloud condensation nuclei in the Amazon rain forest – Part 1: Aerosol size distribution, hygroscopicity, and new model parametrizations for CCN prediction, *Atmospheric Chemistry and Physics*, 16, 15 709–15 740, <https://doi.org/10.5194/acp-16-15709-2016>, 2016.
- 15 Quinn, P. K., Bates, T. S., Coffman, D. J., and Covert, D. S.: Influence of particle size and chemistry on the cloud nucleating properties of aerosols, *Atmospheric Chemistry and Physics*, 8, 1029–1042, <https://doi.org/10.5194/acp-8-1029-2008>, 2008.
- Reid, J. S., Hobbs, P. V., Rangno, A. L., and Hegg, D. A.: Relationships between cloud droplet effective radius, liquid water content, and droplet concentration for warm clouds in Brazil embedded in biomass smoke, *Journal of Geophysical Research: Atmospheres*, 104, 6145–6153, <https://doi.org/10.1029/1998JD200119>, 1999.
- 20 Reisin, T. G., Yin, Y., Levin, Z., and Tzivion, S.: Development of giant drops and high-reflectivity cores in Hawaiian clouds: numerical simulations using a kinematic model with detailed microphysics, *Atmospheric Research*, 45, 275 – 297, [https://doi.org/10.1016/S0169-8095\(97\)00081-1](https://doi.org/10.1016/S0169-8095(97)00081-1), 1998.
- 25 Reutter, P., Su, H., Trentmann, J., Simmel, M., Rose, D., Gunthe, S. S., Wernli, H., Andreae, M. O., and Pöschl, U.: Aerosol- and updraft-limited regimes of cloud droplet formation: influence of particle number, size and hygroscopicity on the activation of cloud condensation nuclei (CCN), *Atmospheric Chemistry and Physics*, 9, 7067–7080, <https://doi.org/10.5194/acp-9-7067-2009>, 2009.
- Rissman, T. A., Nenes, A., and Seinfeld, J. H.: Chemical Amplification (or Dampening) of the Twomey Effect: Conditions Derived from Droplet Activation Theory, *Journal of the Atmospheric Sciences*, 61, 919–930, [https://doi.org/10.1175/1520-0469\(2004\)061<0919:CAODOT>2.0.CO;2](https://doi.org/10.1175/1520-0469(2004)061<0919:CAODOT>2.0.CO;2), 2004.
- 30 Roesler, E. L. and Penner, J. E.: Can global models ignore the chemical composition of aerosols?, *Geophysical Research Letters*, 37, <https://doi.org/10.1029/2010GL044282>, 2010.
- Rose, D., Nowak, A., Achtert, P., Wiedensohler, A., Hu, M., Shao, M., Zhang, Y., Andreae, M. O., and Pöschl, U.: Cloud condensation nuclei in polluted air and biomass burning smoke near the mega-city Guangzhou, China – Part 1: Size-resolved measurements and implications for the modeling of aerosol particle hygroscopicity and CCN activity, *Atmospheric Chemistry and Physics*, 10, 3365–3383, <https://doi.org/10.5194/acp-10-3365-2010>, 2010.
- Rosenfeld, D., Lohmann, U., Raga, G. B., O'Dowd, C. D., Kulmala, M., Fuzzi, S., Reissell, A., and Andreae, M. O.: Flood or Drought: How Do Aerosols Affect Precipitation?, *Science*, 321, 1309–1313, <https://doi.org/10.1126/science.1160606>, 2008.



- Rotach, M. W. and Zardi, D.: On the boundary-layer structure over highly complex terrain: Key findings from MAP, *Quarterly Journal of the Royal Meteorological Society*, 133, 937–948, <https://doi.org/10.1002/qj.71>, 2007.
- Sánchez Gácita, M., Longo, K. M., Freire, J. L. M., Freitas, S. R., and Martin, S. T.: Impact of mixing state and hygroscopicity on CCN activity of biomass burning aerosol in Amazonia, *Atmospheric Chemistry and Physics*, 17, 2373–2392, <https://doi.org/10.5194/acp-17-2373-2017>, 2017.
- Seifert, A. and Beheng, K. D.: A two-moment cloud microphysics parameterization for mixed-phase clouds. Part 2: Maritime vs. continental deep convective storms, *Meteorology and Atmospheric Physics*, 92, 67–82, <https://doi.org/10.1007/s00703-005-0113-3>, 2006.
- Shipway, B. J. and Hill, A. A.: Diagnosis of systematic differences between multiple parametrizations of warm rain microphysics using a kinematic framework, *Quarterly Journal of the Royal Meteorological Society*, 138, 2196–2211, <https://doi.org/10.1002/qj.1913>, 2012.
- 10 Stevens, B., Feingold, G., Cotton, W. R., and Walko, R. L.: Elements of the Microphysical Structure of Numerically Simulated Nonprecipitating Stratocumulus, *Journal of the Atmospheric Sciences*, 53, 980–1006, [https://doi.org/10.1175/1520-0469\(1996\)053<0980:EOTMSO>2.0.CO;2](https://doi.org/10.1175/1520-0469(1996)053<0980:EOTMSO>2.0.CO;2), 1996.
- Sun, J., Leighton, H., Yau, M. K., and Ariya, P.: Numerical evidence for cloud droplet nucleation at the cloud-environment interface, *Atmospheric Chemistry and Physics*, 12, 12 155–12 164, <https://doi.org/10.5194/acp-12-12155-2012>, 2012.
- 15 Twomey, S.: Pollution and the planetary albedo, *Atmospheric Environment* (1967), 8, 1251 – 1256, [https://doi.org/10.1016/0004-6981\(74\)90004-3](https://doi.org/10.1016/0004-6981(74)90004-3), 1974.
- Tzivion, S., Feingold, G., and Levin, Z.: An Efficient Numerical Solution to the Stochastic Collection Equation, *Journal of the Atmospheric Sciences*, 44, 3139–3149, [https://doi.org/10.1175/1520-0469\(1987\)044<3139:AENSTT>2.0.CO;2](https://doi.org/10.1175/1520-0469(1987)044<3139:AENSTT>2.0.CO;2), 1987.
- Tzivion, S., Feingold, G., and Levin, Z.: The Evolution of Raindrop Spectra. Part II: Collisional Collection/Breakup and Evaporation in a Rainshaft, *Journal of the Atmospheric Sciences*, 46, 3312–3328, [https://doi.org/10.1175/1520-0469\(1989\)046<3312:TEORSP>2.0.CO;2](https://doi.org/10.1175/1520-0469(1989)046<3312:TEORSP>2.0.CO;2), 1989.
- 20 Wang, J., Krejci, R., Giangrande, S., Kuang, C., Barbosa, H. M. J., Brito, J., Carbone, S., Chi, X., Comstock, J., Ditas, F., Lavric, J., Manninen, H. E., Mei, F., Moran-Zuloaga, D., Pöhlker, C., Pöhlker, M. L., Saturno, J., Schmid, B., Souza, R. A. F., Springston, S. R., Tomlinson, J. M., Toto, T., Walter, D., Wimmer, D., Smith, J. N., Kulmala, M., Machado, L. A. T., Artaxo, P., Andreae, M. O., Petäjä, T., and Martin, S. T.: Amazon boundary layer aerosol concentration sustained by vertical transport during rainfall, *Nature*, 539, 416–419, <https://doi.org/10.1038/nature19819>, 2016.
- 25 Ward, D. S., Eidhammer, T., Cotton, W. R., and Kreidenweis, S. M.: The role of the particle size distribution in assessing aerosol composition effects on simulated droplet activation, *Atmospheric Chemistry and Physics*, 10, 5435–5447, <https://doi.org/10.5194/acp-10-5435-2010>, 2010.
- 30 Wendisch, M., Pöschl, U., Andreae, M. O., Machado, L. A. T., Albrecht, R., Schlager, H., Rosenfeld, D., Martin, S. T., Abdelmonem, A., Afchine, A., Araújo, A. C., Artaxo, P., Aufmhoff, H., Barbosa, H. M. J., Borrmann, S., Braga, R., Buchholz, B., Cecchini, M. A., Costa, A., Curtius, J., Dollner, M., Dorf, M., Dreiling, V., Ebert, V., Ehrlich, A., Ewald, F., Fisch, G., Fix, A., Frank, F., Fütterer, D., Heckl, C., Heidelberg, F., Hüneke, T., Jäkel, E., Järvinen, E., Jurkat, T., Kanter, S., Kästner, U., Kenntner, M., Kesselmeier, J., Klimach, T., Knecht, M., Kohl, R., Kölling, T., Krämer, M., Krüger, M., Krisna, T. C., Lavric, J. V., Longo, K., Mahnke, C., Manzi, A. O., Mayer, B., Mertes, S., Minikin, A., Mollleker, S., Münch, S., Nillius, B., Pfeilsticker, K., Pöhlker, C., Roiger, A., Rose, D., Rosenow, D., Sauer, D., Schnaiter, M., Schneider, J., Schulz, C., de Souza, R. A. F., Spanu, A., Stock, P., Vila, D., Voigt, C., Walser, A., Walter, D., Weigel, R., Weinzierl, B., Werner, F., Yamasoe, M. A., Ziereis, H., Zinner, T., and Zöger, M.: ACRIDICON–CHUVA Campaign: Studying Tropical



- Deep Convective Clouds and Precipitation over Amazonia Using the New German Research Aircraft HALO, *Bulletin of the American Meteorological Society*, 97, 1885–1908, <https://doi.org/10.1175/BAMS-D-14-00255.1>, 2016.
- Yin, Y., Levin, Z., Reisin, T., and Tzivion, S.: The effects of giant cloud condensation nuclei on the development of precipitation in convective clouds — a numerical study, *Atmospheric Research*, 53, 91 – 116, [https://doi.org/10.1016/S0169-8095\(99\)00046-0](https://doi.org/10.1016/S0169-8095(99)00046-0), 2000a.
- 5 Yin, Y., Levin, Z., Reisin, T., and Tzivion, S.: Seeding Convective Clouds with Hygroscopic Flares: Numerical Simulations Using a Cloud Model with Detailed Microphysics, *Journal of Applied Meteorology*, 39, 1460–1472, [https://doi.org/10.1175/1520-0450\(2000\)039<1460:SCCWHF>2.0.CO;2](https://doi.org/10.1175/1520-0450(2000)039<1460:SCCWHF>2.0.CO;2), 2000b.

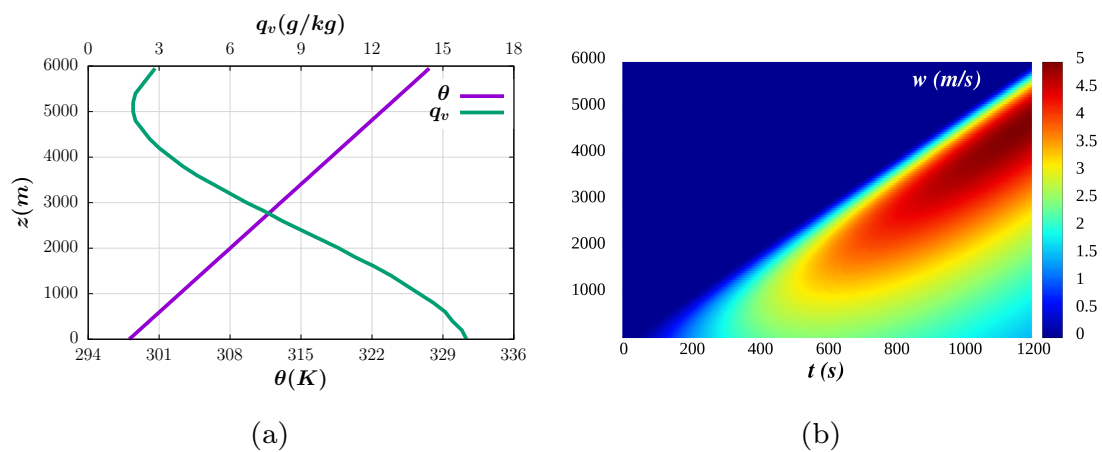


**Figure 1.** Model configuration: (a) initial conditions and (b) prescribed field of vertical velocity



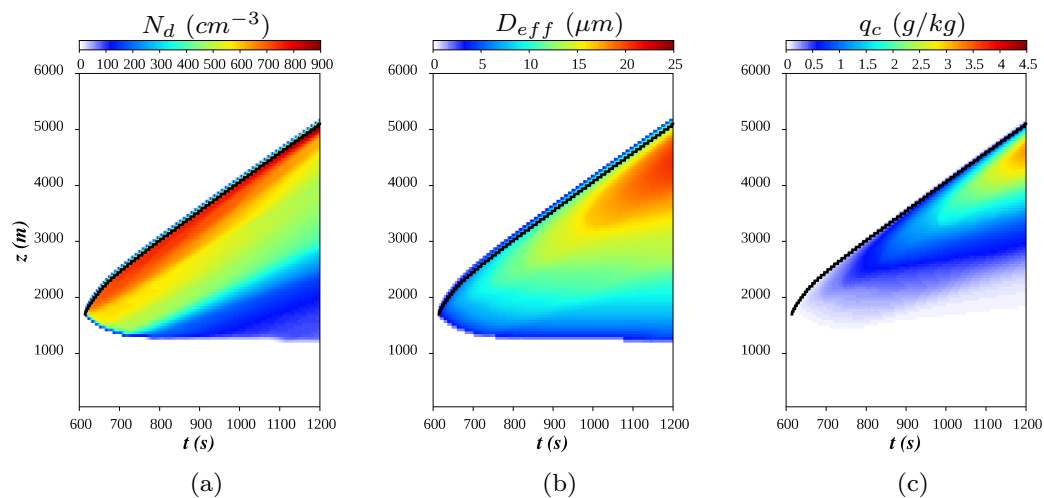


**Figure 2.** Evolution of  $N_d$  ( $\text{cm}^{-3}$ ),  $D_{eff}$  ( $\mu\text{m}$ ) and  $q_c$  ( $\text{g/kg}$ ) in the simulation. The black lines represent cloud-top.

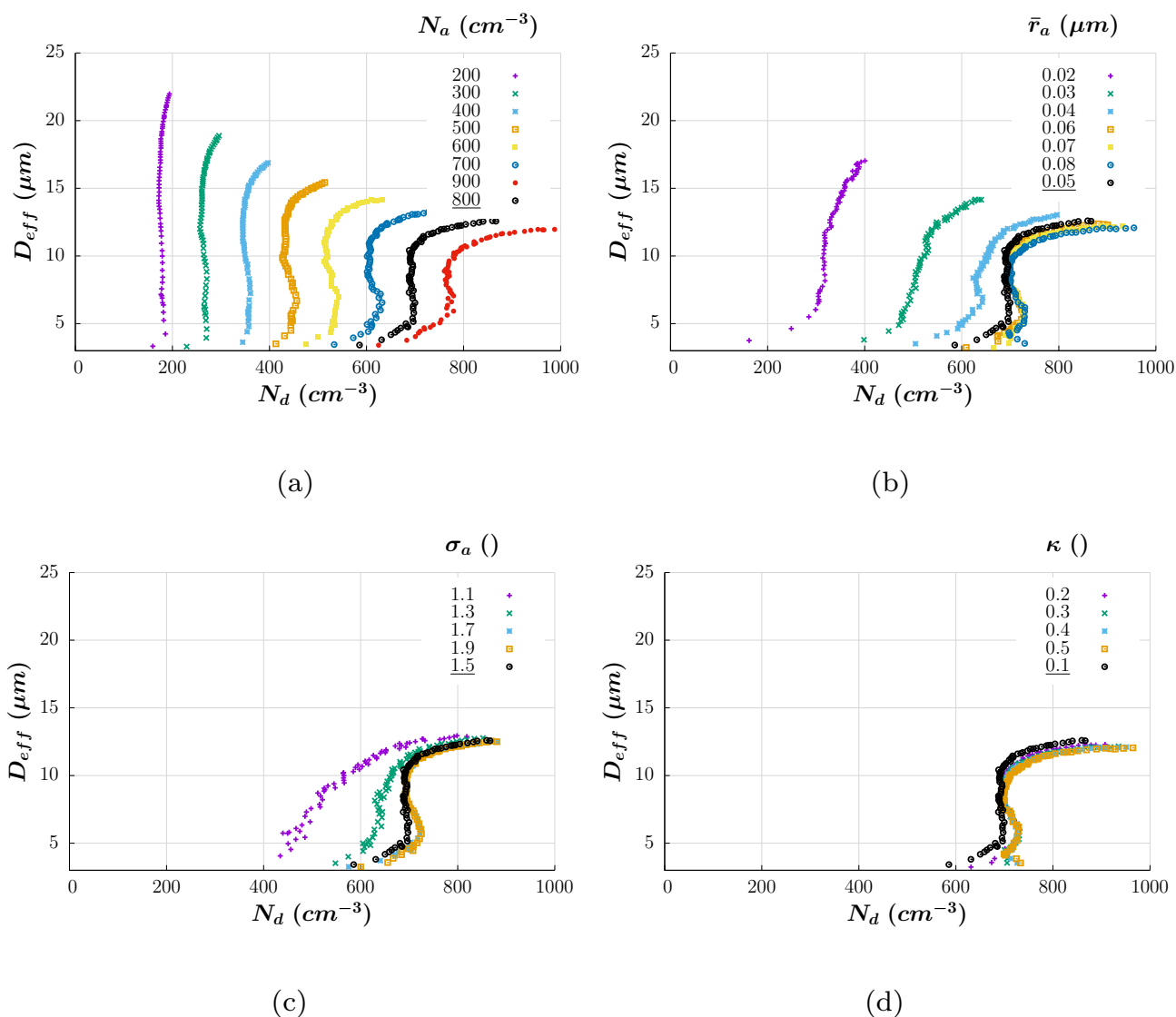


**Figure 3.** Illustration of the sensitivity of cloud-top bulk properties to (a) the aerosol number concentration ( $cm^{-3}$ ), (b) the median radius of the aerosol size distribution ( $\mu m$ ), (c) the geometric standard deviation of the aerosol size distribution (dimensionless), and (d) the aerosol hygroscopicity (dimensionless). The markers represent the averaged DSDs for the time steps when the cloud top remains at the same model level during its growth. The colors distinguish between simulations using different values of the parameter specified at the top of the graphs. The control simulation is represented by black markers in the figures.

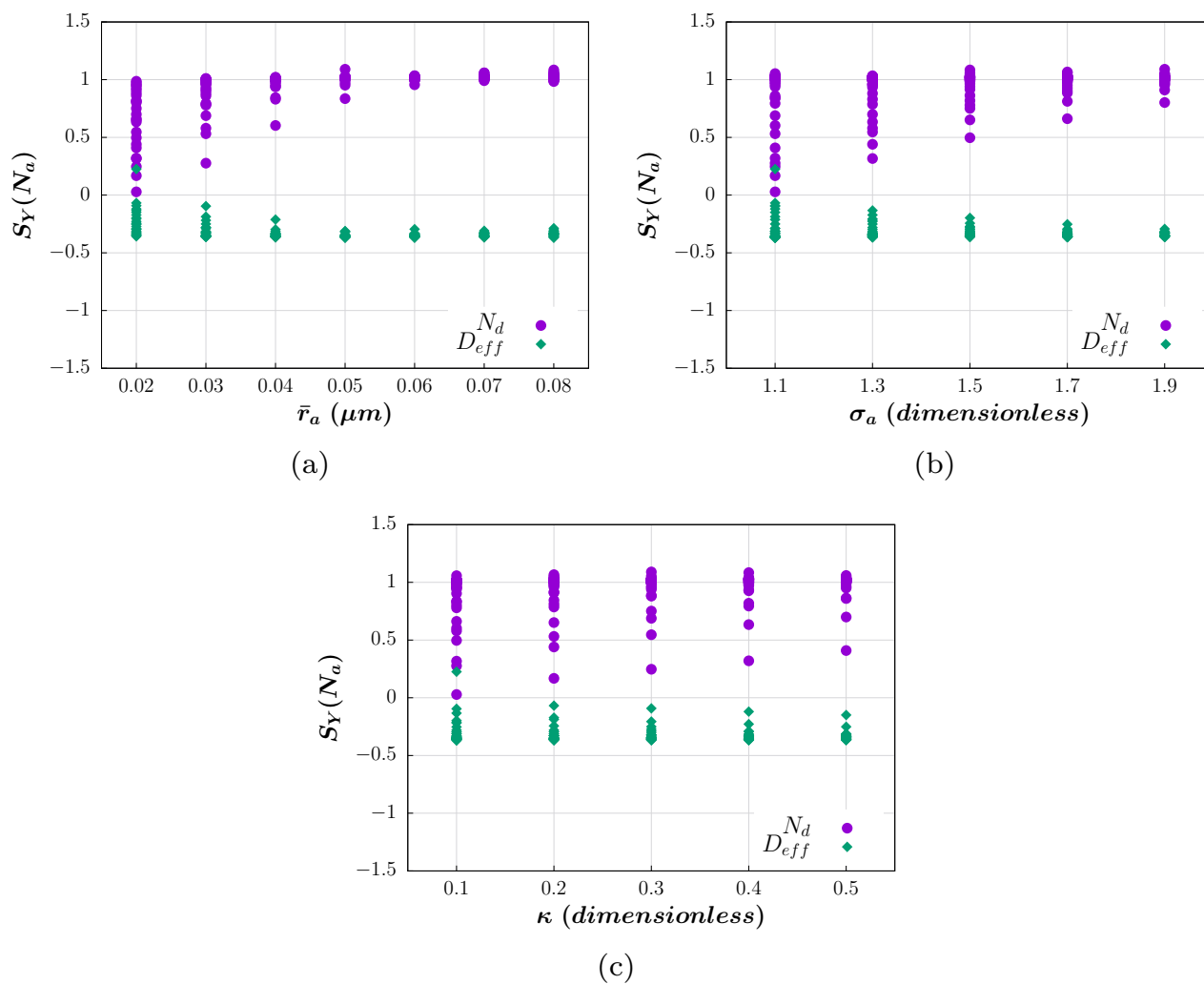


**Figure 4.** Sensitivities of the droplet number concentration and effective diameter to the aerosol number concentration ( $S_Y(N_a)$ ) as a function of (a) the median radius of the aerosol size distribution ( $\mu\text{m}$ ), (b) the geometric standard deviation of the aerosol size distribution (dimensionless) and (c) the aerosol hygroscopicity (dimensionless).

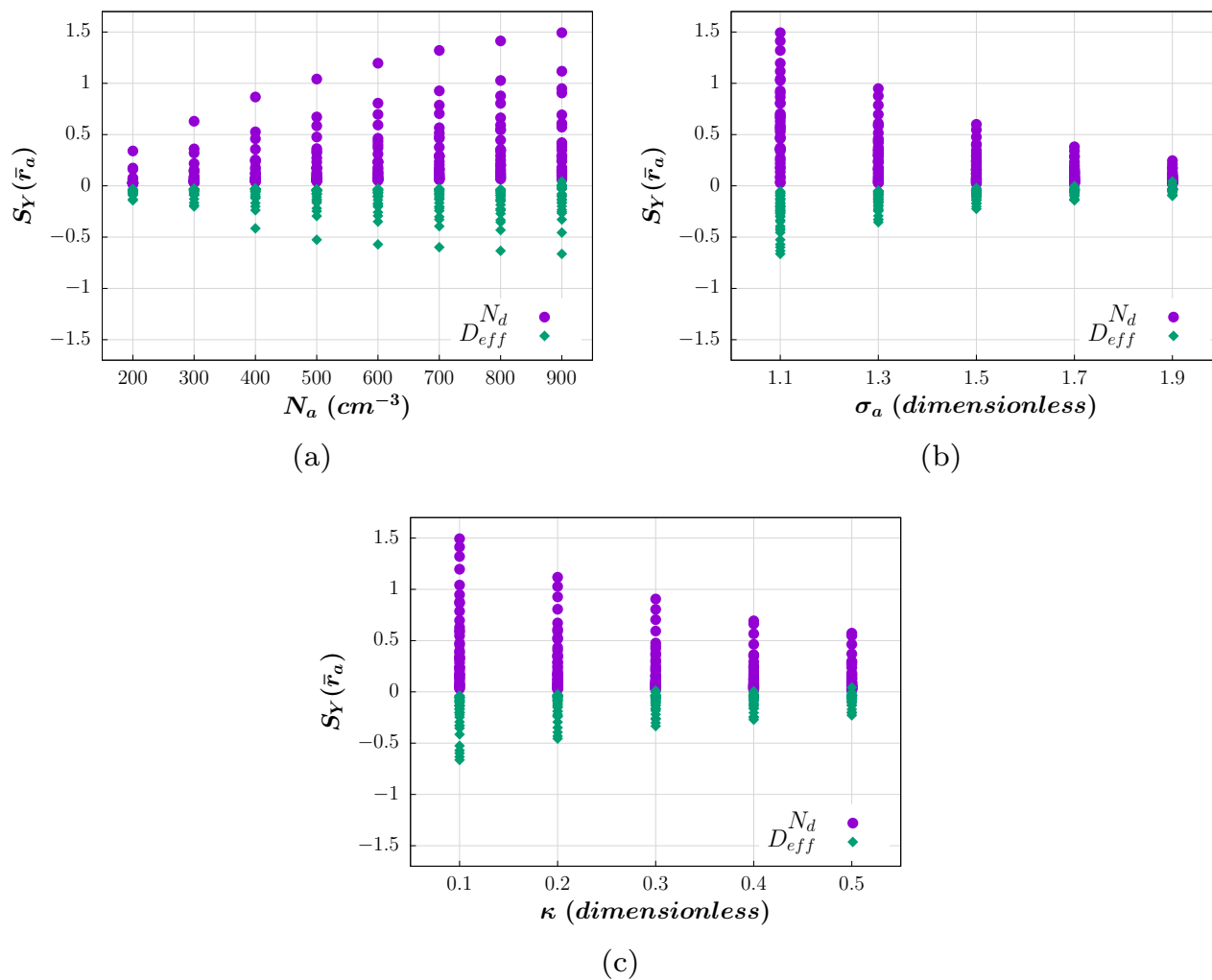


**Figure 5.** Sensitivities of the droplet number concentration and effective diameter to the median radius of the aerosol size distribution ( $S_Y(\bar{r}_a)$ ) as a function of (a) the aerosol number concentration ( $cm^{-3}$ ), (b) the geometric standard deviation of the aerosol size distribution (dimensionless) and (c) the aerosol hygroscopicity (dimensionless).

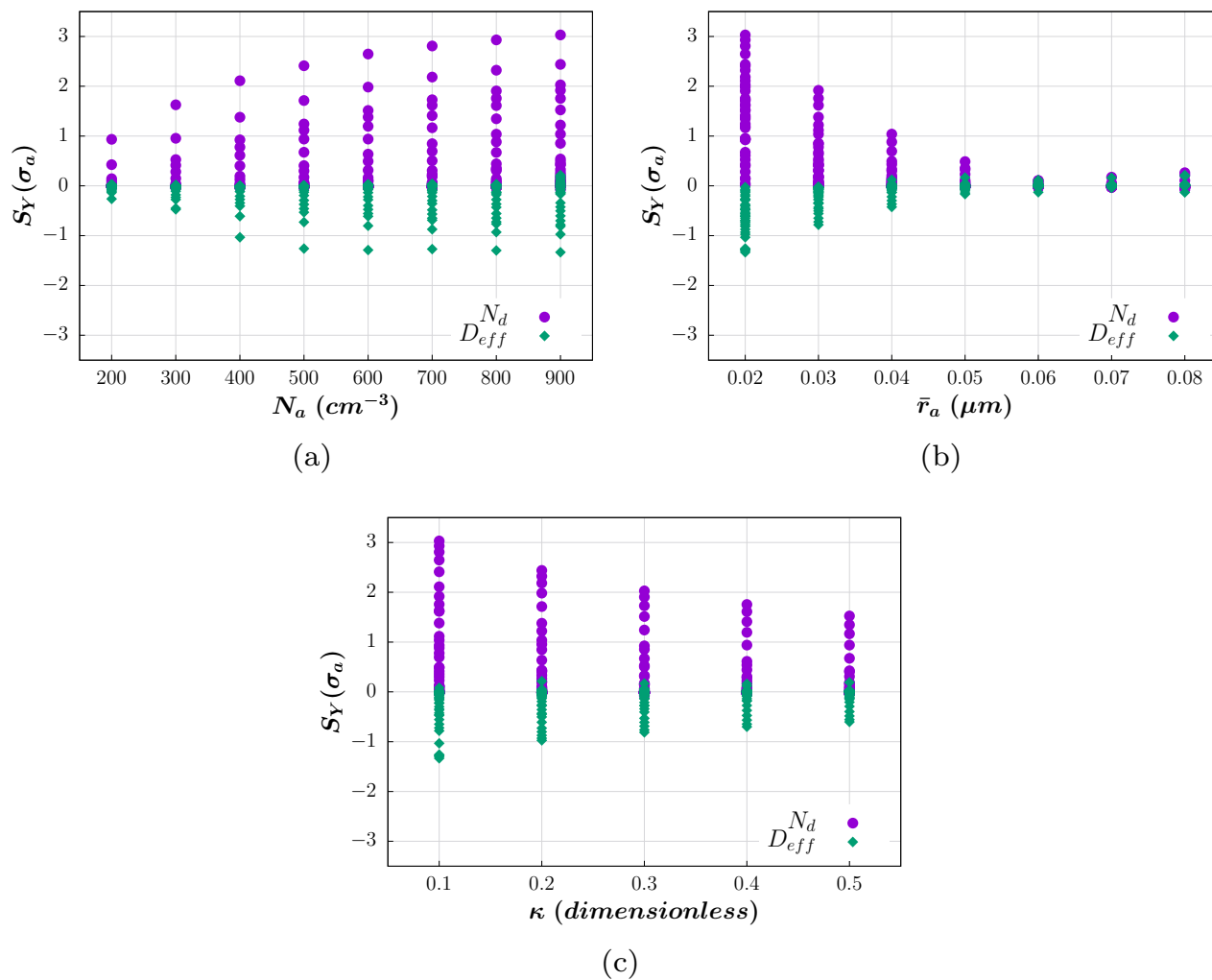


**Figure 6.** Sensitivities of the droplet number concentration and effective diameter to the geometric standard deviation of the aerosol size distribution ( $S_Y(\sigma_a)$ ) as a function of (a) the aerosol number concentration ( $cm^{-3}$ ), (b) the median radius of the aerosol size distribution ( $\mu m$ ) and (c) the aerosol hygroscopicity (dimensionless).

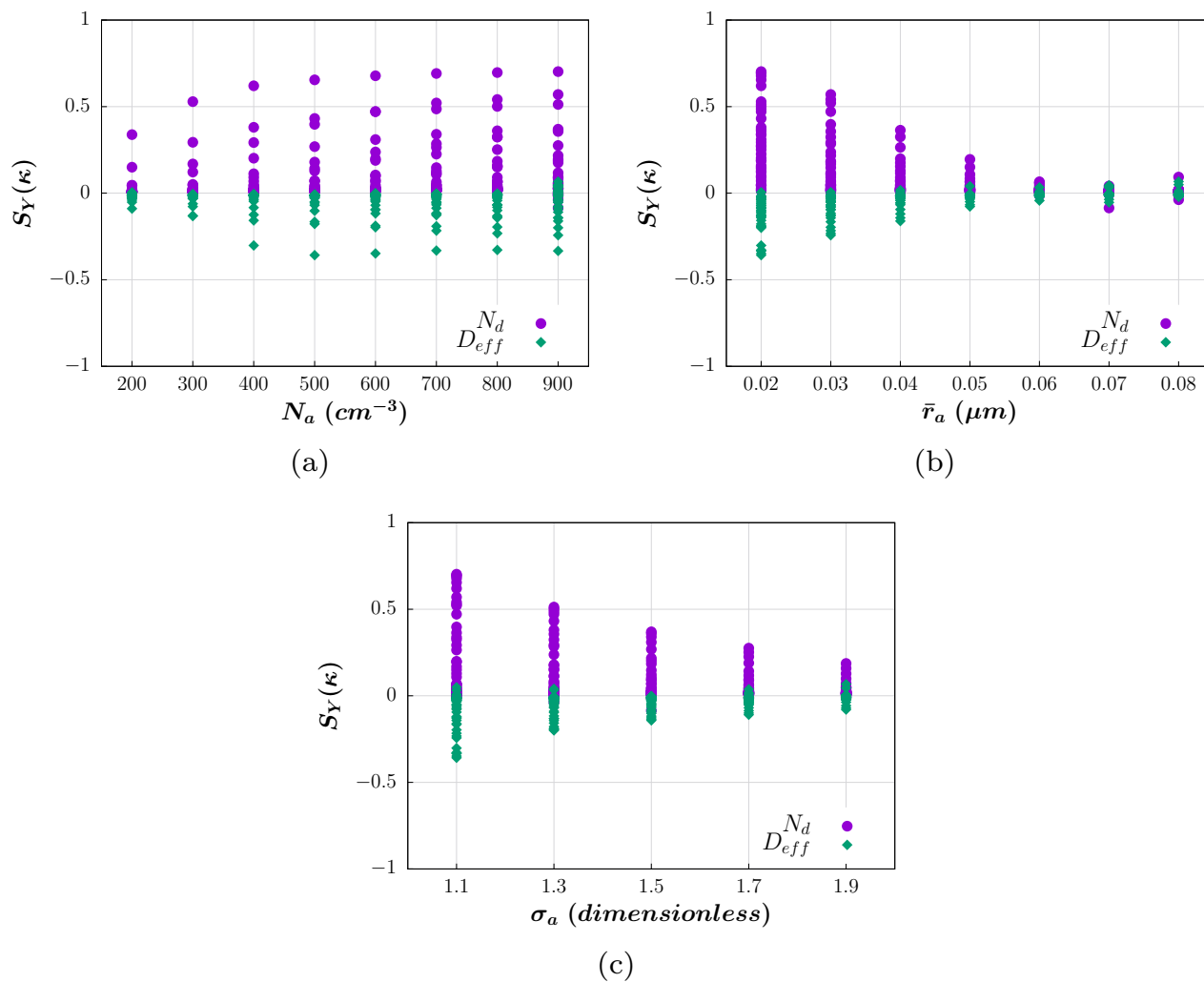


**Figure 7.** Sensitivities of the droplet number concentration and effective diameter to the aerosol hygroscopicity ( $S_Y(\kappa)$ ) as a function of (a) the aerosol number concentration ( $cm^{-3}$ ), (b) the median radius of the aerosol size distribution ( $\mu m$ ) and (c) the geometric standard deviation of the aerosol size distribution (dimensionless).

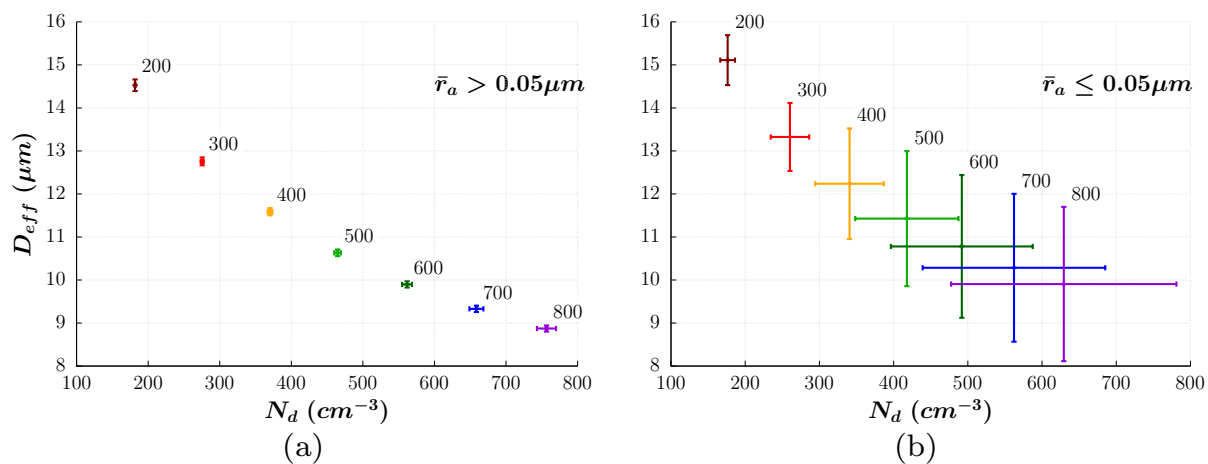


**Figure 8.** Mean and standard deviation of the time-averaged values of  $N_d$  and  $D_{eff}$  at the cloud top for each simulation.